Stimulated emission of 0.2-THz phonons in $LaF_3:Er^{3+}$

D. J. Sox, J. E. Rives, and R. S. Meltzer
Department of Physics and Astronomy, University of Georgia, Athens, Georgia 30602
(Received 21 September 1981)

Stimulated emission of phonons in the 0.2-THz frequency range is observed in $LaF_3:Er^{3+}$. The phonons are generated in the relaxation between the Kramers components of the $^4S_{3/2}(1)$ state of Er^{3+} split in a magnetic field after inverting the population with a pulsed tunable dye laser. The stimulated emission is identified from the temporal behavior of the luminescence from the upper Kramers component which shows a speedup in the relaxation during inversion. The population dynamics are analyzed with the rate equations for the system. Comparison with experiment indicates strong preferential stimulated emission along the axis of the cylindrically excited volume and a gain of up to 5 mm^{-1}. The population inversion exists sufficiently long for phonon propagation over macroscopic distances and the phonon frequency is tunable with the magnetic field.

I. INTRODUCTION

Phonons, as quantum excitations of the phonon field, behave much the same as do photons, quantum excitations of the electromagnetic field. Stimulated emission, for example, has been observed for the phonon field on several occasions, although to our knowledge a resonant phonon cavity has not been established. Stimulated emission at microwave frequencies (5—30 GHz), also known as the phonon avalanche,[1] has been studied in several systems and the nonlinear behavior has been treated theoretically.[2,3] Typically, an ion with a degenerate ground state is split in an external magnetic field and the population is inverted by some means. The inverted population remains nearly constant for a short period of time (usually ~ 1 μs) until stimulated emission takes over bringing the system to saturation ($\sim 10-100$ μs). The populations then continue to thermalize at a rate T_1^{-1} ($\sim 10^3$/s) or slower if the resonant phonon population becomes bottlenecked.

More recently, stimulated phonon emission has been observed at much higher (~ 1 THz) frequencies. Grill and Bron[4] found evidence for stimulated emission of 24-cm^{-1} (0.72-THz) phonons in $Al_2O_3:V^{4+}$ using infrared excitation of a three-level system. Phonons were detected with a superconducting Sn bolometer which showed a signal with a characteristic threshold and nonlinear behavior. In this system T_1 is very short (~ 0.1 ns). Similarly, evidence for stimulated emission of 29-cm^{-1} (0.87-THz) phonons in ruby has been presented by Hu.[5] In this system optical excitation was used to invert the population of the ^2E pair of excited states and nonlinear phonon emission was detected with a granular Al superconducting bolometer. The stimulated phonon emission was seen exclusively within a 6° cone directed along the c axis. In this system T_1 is also quite short (1.1 ns).[6]

In the present work we discuss the results of experiments which indicate the existence of strong stimulated phonon emission at $3-7.5$ cm^{-1} ($0.09-0.22$ THz). Three important differences between these experiments and the previous high-frequency work are (1) T_1 for the present system is much longer ($\sim 0.1-100$ μs), (2) the phonon frequency is readily tunable from $\sim 3-20$ cm^{-1} ($0.1-0.6$ THz) with a magnetic field up to 85 kG, and (3) evidence for the stimulated emission is obtained directly by monitoring the populations of the electronic states resonant with the phonons.

The excited-state populations and phonon dynamics are described with rate equations. A comparison of the rate equations with experiments enables us to determine some fundamental parameters describing the electron-phonon system. The analysis suggests strong stimulated emission occurring predominantly along the axis of the optically excited volume.

II. EXPERIMENTAL TECHNIQUES

The population inversion is obtained by pumping the upper component of the $^4S_{3/2}(1)$ Kramers pair, split with an external magnetic field H along the c axis, as shown in Fig. 1. The dynamics of these

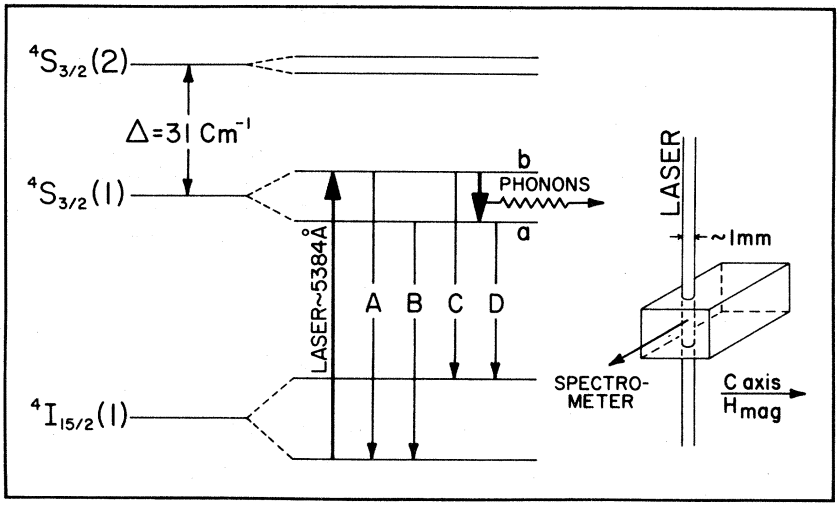

FIG. 1. Relevant energy levels of Er^{3+} in LaF_3 split in an external magnetic field along the c axis. Stimulated emission of phonons occurs in the relaxation $b \rightarrow a$ after inverting the population with a laser pulse. The experimental geometry is shown on the right.

states have been studied by Broer *et al.*[7] at low fields and by Wolfrum, Lanzinger, and Renk[8] at higher magnetic fields. At high fields, the spin-lattice relaxation is governed by a single phonon process and its rate T_1^{-1} is proportional to H^5. At low fields (<8 kG) cross relaxation dominates at low temperatures while at higher temperatures, an Orbach process involving coupling to the $^4S_{3/2}(2)$ pair of states $\Delta=31$ cm^{-1} above $^4S_{3/2}(1)$ becomes prevalent ($T_1^{-1}=2.4\times10^{10}e^{-\Delta/kT}$ s^{-1}).

The experiments were carried out on a sample of 0.1% LaF_3:Er^{3+} (Optovac, Inc.) in magnetic fields between 15—28.0 kG. The samples were typically 0.5—1 cm on a side. Excitation was accomplished with either a Nd:YAG (yttrium aluminum garnet) pumped tunable dye laser producing 5-ns, 0.3-cm^{-1} bandwidth pulses containing up to 7 mJ of energy or a coaxial flash-lamp-pumped tunable dye laser with ~500-ns, 0.4-cm^{-1} bandwidth pulses at energies up to 30 mJ. A total population inversion within the two Kramers components of $^4S_{3/2}(1)$, split in a magnetic field, was obtained by tuning the laser to the upper Zeeman level at ~5384 Å.

The excited state populations were monitored from the emissions labeled C and D in Fig. 1 using a 1.8-m Ebert spectrometer at a (2—3)-cm^{-1} spectral resolution. The emission was detected on a cooled fast photomultiplier (Amperex TVP 56) and the time dependence of the photomultiplier output was recorded directly on a transient digitizer (Biomation 6500). Data from each of 25—500 single shots were transferred digitally to a multichannel analyzer for signal averaging. Because of the close spectral proximity of the laser pulse and emission the sample was carefully masked to minimize scattered laser light.

III. EXPERIMENTAL RESULTS

T_1 was first measured at several magnetic fields using a N_2-pumped tunable dye laser with 50-μJ excitation pulses and was found to be consistent with the work of Wolfrum, Lanzinger, and Renk.[8] The decay obtained from the time dependence of the intensity of transition C (upper state) is exponential as shown by curves I in Figs. 2 (20.2 kG) and 3 (28.5 kG) with decay times of 46 and 6.2 μs, respectively. Under conditions of much higher excitation pulse energies obtained with the Nd:YAG-pumped dye laser, nonexponential behavior is obtained at 20.2 kG as shown in curves II and III of Fig. 2. In these experiments the laser was focused to a ~1.5×2-mm^2 rectangle, exciting a 5-mm length of crystal. Based on the measured absorption to the upper Zeeman level ($\alpha=0.21$ cm^{-1}) we estimate a maximum N^* (3.5 mJ at sample) of $\simeq5\times10^{16}$ cm^{-3}. The decay of the upper state exhibits the following characteristics. (1) There is a noticeable speed-up at early times followed by (2) a slowing down of the decay at long times ($t > T_1$) with both effects becoming more pronounced at higher excitation energies. (3) The crossover between the region of enhanced and reduced decay rates always occurs near saturation, and (4) there is an initial delay period ($t << T_1$)

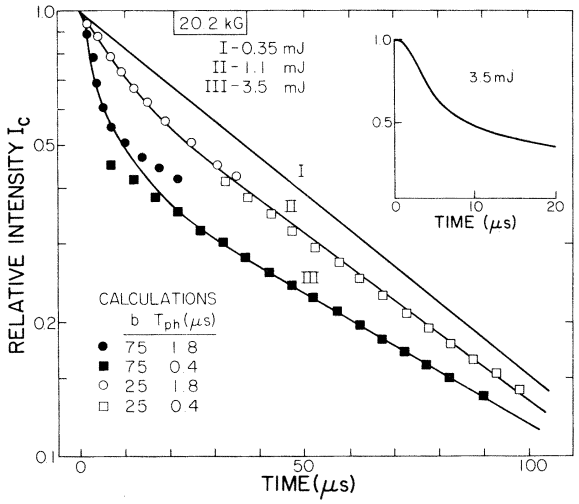

FIG. 2. Experimental (solid curves) and calculated (points) time dependence of the emission (transition C) which is proportional to the population of state b. The $LaF_3:Er^{3+}$ sample was in a magnetic field of 20.2 kG. The insert shows the initial delay seen with higher time resolution.

during which the decay proceeds at a rate $\sim T_1^{-1}$ before the enhanced decay takes over as can be seen in the insert of Fig. 2. Similar conclusions follow from data taken at 28.5 kG using the flash-lamp-pumped tunable dye laser focused to a 800-μm diameter spot ($N^*_{max} \simeq 8\times 10^{17}$ cm^{-3} with 17 mJ at sample) as shown in Fig. 3. The data at 28.5 kG exhibit a rounded maximum due to the

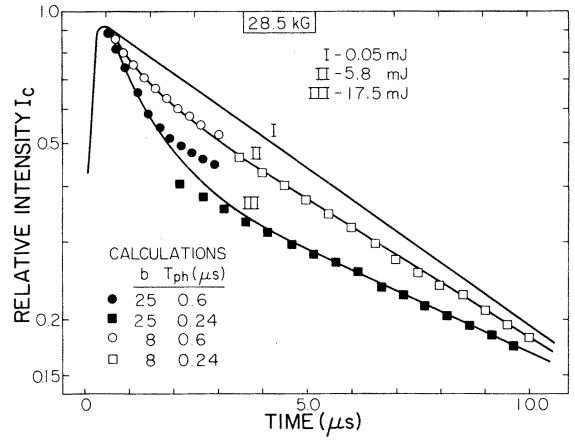

FIG. 3. Experimental (solid curves) and calculated (points) time dependence of the emission (transition C) in $LaF_3:Er^{3+}$ in a magnetic field of 28.5 kG.

much longer excitation pulse ($\simeq$500 ns) of the flash-lamp-pumped tunable dye laser and therefore do not show the initial decay rate of T_1^{-1}.

Laser heating of the samples was observed in some experiments. Laser heating can lead to Orbach relaxation involving the $^4S_{3/2}(2)$ state 31-cm^{-1} higher in energy and a large background luminescence from the upper Zeeman level. The amount of heating depends upon the laser energy, surface condition, absorption strength of the transition in resonance with the laser, absorption path, and volume of the sample. The temperature is estimated from the relative intensity ratio of emission from the upper state (transition C) to that of the lower state (transition D), corrected for the 5 times greater transition strength of C relative to D. Where resonantly generated phonons are produced (excitation of the upper state) the intensity ratio is obtained after thermalization has been achieved ($\sim$25 μs).

Excitation of the smaller samples ($7\times 7\times 3$ mm^3) into the lower state (stronger absorption) with 10 mJ produced temperatures of $\sim$5.3 K. When excitation occurred to the upper state the sample temperature reached $\sim$4 K, probably due to the reduced absorption. However, this was sufficient to produce an Orbach-dominated relaxation time of 2.5 μs, as evidenced by its exponential character, which is consistent with the Orbach relaxation rate

$$T_1^{-1}(\text{orb}) = 2.4\times 10^{10} e^{-\Delta/kT}\ \text{s}^{-1}$$

$$= 3.1\times 10^5\ \text{s}^{-1}$$

expected at $T=4$ K.[7] However, when a $7\times 7\times 7$-mm^3 sample or $7\times 7\times 15$-mm^3 sample was excited into the lower state with 17.5 mJ, temperatures of 3.2 and 2.8 K, respectively, were observed because of the large sample volumes. At these temperatures the Orbach relaxation does not compete with the single-phonon-induced stimulated emission and nonexponential decay due to stimulated emission is observed. Thus it is imperative to work with large samples to avoid problems associated with laser heating.

The energy source of the heating cannot be the 7-cm^{-1} resonantly generated phonons ($\sim 10^{-8}$ J) but probably results from a combination of multiphonon relaxation from $^4S_{3/2}$ to $^4F_{9/2}$ and heating at the sample surfaces. If we let the multiphonon relaxation occur at the expected rate of $\sim 10^2$/s,[9] the decay is equivalent to a thermal power input to the sample of $\sim$10 mW.

IV. THEORY

A. Estimate of stimulated emission

Before we examine the rate equations we ask whether it is reasonable to expect stimulated emission under the conditions of these experiments? We first estimate the mean free path Λ_{res} for stimulated phonon emission or absorption given by

$$\Lambda_{res}=v_0\tau_{res}=\frac{v_0 T_1 \Sigma}{N^*} , \tag{1}$$

where v_0 is the speed of sound (2.7×10^5 cm/s for transverse phonons[10]), τ_{res} is the time between resonant scattering events, and Σ is the density of phonon modes within the phonon resonance.

If we assume a resonance width of 100 MHz ($\sim$14 G), typical of spin-resonance linewidths for rare-earth ions, we find $\Sigma\simeq6\times10^{15}$ cm^{-3} at 0.22 THz. Thus, for the maximum value of N^* in these experiments at 28.5 kG ($\sim10^{18}$ cm^{-3}), $\Lambda_{res}=800$ μm, which is approximately the diameter of the excited volume. Since $\tau_{res}<<T_1$, the population inversion is maintained during the phonon transit time across the excited volume, allowing for stimulated phonon emission. Phonons traveling along the axis of the cylindrical volume ($\sim$5-mm long) can of course traverse many mean free paths in a single pass. Thus it appears that the observation of stimulated emission is reasonable.

B. Rate equations

Spin-lattice relaxation between two electronic states in the presence of phonon bottlenecking can be described by the rate equations:

$$\frac{dn_1}{dt}=T_1^{-1}[(1+\bar{p})n_2-\bar{p}n_1] , \tag{2a}$$

$$\frac{dn_2}{dt}=-\frac{dn_1}{dt} , \tag{2b}$$

$$\frac{d\bar{p}}{dt}=-T_{ph}^{-1}\bar{p}+\frac{N^*}{\Sigma}\frac{dn_1}{dt} , \tag{2c}$$

where n_2 and n_1 are the relative populations of the upper and lower states N_1/N^* and N_2/N^*, respectively, $\bar{p}$ is the average phonon occupation number within the resonance width, and T_{ph} is the phonon lifetime within the optically excited volume.

In the absence of phonon bottlenecking ($\bar{p}<<1$) Eqs. (2) predict the usual exponential decay at a rate T_1^{-1}. Brya and Wagner[1] showed that the rate equations provide a semiquantitative description of the behavior of the spin system under strong bottlenecking conditions and an initially inverted population. Considerations of spatial and spectral transport may also be necessary to give good quantitative agreement.[2] Furthermore, due to their statistical nature, conditions exist under which the rate equations have limited validity. Leonardi and Persico,[3] using a microscopic approach, have shown that there is a time-dependent phonon band narrowing under avalanche conditions (inverted population) which is not described in Eqs. (2). In addition it is not always possible to describe the resonant phonon loss in terms of a simple loss rate T_{ph}^{-1} as in Eq. (2c).

However, under the present conditions of moderately strong bottlenecking we expect that the rate equations should provide at least a semiquantitative description of the behavior of the spin-phonon system. With an initially inverted population ($n_2>n_1$) and $b=N^*/\Sigma>>1$ the rate equations predict an initial decay of n_2 at the rate T_1^{-1}. The phonon population eventually builds up to the point where stimulated emission predominates causing a phonon avalanche and n_2 decays at a rate faster than T_1^{-1} until saturation is reached. At times which are long compared to the time to reach saturation the decay proceeds at the much slower bottlenecked decay rate $[T_1+(1+b)T_{ph}]^{-1}$. For a given T_1^{-1} both the avalanche decay rate and the bottlenecked regime decay rate depend on the bottleneck factor b and the phonon loss rate T_{ph}^{-1}. Under the conditions of these experiments where $T_{ph}<<T_1$, the decay rate in the avalanche regime is proportional to bT_{ph} whereas in the bottlenecked regime the decay rate is proportional to $(bT_{ph})^{-1}$. T_{ph} is determined by the time for spatial escape of the phonons from the excited volume since anharmonic decay times at 0.2 THz are estimated to be much greater.[11]

C. Comparison to experiment

Comparisons of the computer solutions from the rate equations with experiment are not expected to provide quantitative fits to the experimental results for the reasons stated in Sec. IV B. However, the comparison can provide semiquantitative information concerning the magnitude of some of the fundamental parameters used in describing the stimulated emission such as the average mean free path for stimulated emission Λ_{res}, the bottleneck factor $b=N^*/\Sigma$, and the resonance linewidth $\Delta\nu_{res}$.

Attempts to fit the full temporal decay for one magnetic field and laser excitation energy were unsuccessful. It is not possible to describe the early time (inverted population) and later time (well after saturation) behavior with a single value for the parameters b and T_{ph}. We have chosen to describe the temporal response of a single experimental run with a fixed b but two values of T_{ph}, one prior to saturation and one after saturation. The time scale for the computer fits after saturation are shifted to correspond to a new origin so that it coincides with the data. This is empirically successful, except very close to saturation, and one can self-consistently vary b in proportion to laser power with the same two values of T_{ph} for a series of runs at a given magnetic field. This is illustrated in Figs. 2 and 3 for magnetic fields of 20.2 and 28.5 kG, respectively.

There is a sound physical justification for the use of two values for T_{ph}. While the population is inverted stimulated emission dominates the relaxation. As we will show, Λ_{res} is of the order of the radius of the excitation volume. One therefore expects the axially propagating phonon population to dominate the resonant phonon population during strong stimulated emission due to their greater single-pass gain. Ballistic lifetimes appropriate to these phonons are approximately the time required to make a single pass down the axis of the excited volume ($\simeq 2$ μs for a 5-mm path). Well after the excited populations pass through saturation, stimulated emission becomes relatively unimportant and the phonon propagation vectors become random, assuming no anisotropy in the electron-phonon coupling and no phonon focusing. Phonon escape becomes dominated by near-radial motion so the appropriate propagation times become those required to traverse the diameter ($\simeq 0.4$ μs for a 1-mm diameter spot). Values of T_{ph} were selected in this manner for the computer fits and b was varied to obtain the best fits shown in Figs. 2 and 3. We conclude, on the basis of the success of this scheme, that the stimulated emission does indeed show a strong preference for axial propagation.

Values of the experimental parameters and parameters obtained by fitting the data to the rate equation at 20.2 and 28.5 kG are shown in Table I. Included are b_{max}, the maximum values of b, and T_{ph}, the resonant phonon lifetimes before and after saturation, which give the best fits of the rate equations to the observed data shown in Figs. 2 and 3.

The fitted values of T_{ph} before and after saturation for the 20.2-kG runs are consistent, respectively, with the axial (1.8 μs) and radial (0.5 μs) ballistic propagation times for transverse phonons. The fitted values of T_{ph} before and after saturation for 28.5 kG are not totally consistent, respectively, with the axial (1.8 μs) and radial (0.15 μs) ballistic propagation times, particularly that prior to satura-

TABLE I. Experimental, fitted, and calculated values of parameters relevant to stimulated phonon emission in $LaF_3:Er^{3+}$ at 20.2 and 28.5 kOe.

H (kOe)	20.2	28.5
	Experimental parameters	
ν (THz) of phonons	0.15	0.22
spot size (mm)	$1.5\times2\times5$	0.8 (diam)$\times5$
N^*_{max} (cm^{-3})	5×10^{16}	80×10^{16}
	Fitted parameters	
T_1 (μs)	46	6.2
b_{max}	75	25
T_{ph} (μs): before saturation	1.8	0.6
after saturation	0.4	0.24
	Calculated parameters	
τ_{res} (μs)	0.6	0.25
λ_{res} (mm) at N^*_{max}	1.7	0.7
$\Delta\nu_{res}$ (MHz)	25	500

tion, but for 28.5 kG it must be noted that the excited volume has a very small single-pass axial solid angle (9°) limiting the ability of the axial phonons to cause stimulated emission.

From the fitted values of b it is possible to estimate (at the maximum values of N^*) λ_{res} and the resonance width

$$\Delta\nu_{res}=N^*\nu^3/12\pi\nu^2 b \ ,$$

which are listed as calculated parameters in Table I. Note that Λ_{res} at N^*_{max} is of the order of the smallest dimension of the excited volume implying nearly ballistic loss. These values of Λ_{res} indicate large gains in the range of $2-5\ \mathrm{mm}^{-1}$.

The large difference in resonance width $\Delta\nu_{res}$ is rather interesting. Calculation of the field dependence of the inhomogeneous linewidth due to differential admixture of the $^4S_{3/2}(2)$ crystal-field state yields $\Delta\nu \propto H^3$, predicting a threefold increase in the linewidth on going from 20.2 to 28.5 kG, rather than the observed 25-fold increase. Although the relative error in $\Delta\nu_{res}$ at the two fields could be as large as a factor of 2 or 3, a discrepancy remains. It appears, therefore, that the field dependence of the linewidth is more rapid than predicted on the basis of a simple crystal-field theory. Alternatively, anomalies may exist in the phonon density of states at these frequencies.

V. CONCLUSIONS

We have demonstrated the occurrence of strong stimulated emission of high-frequency phonons in $LaF_3:Er^{3+}$. An analysis of the population dynamics using rate equations suggests dominant generation of phonons along the axis of the cylindrically excited volume. The high gain (up to $5\ \mathrm{mm}^{-1}$), long duration of the inverted population ($1-100$ μs) allowing for propagation of the phonons over macroscopic sample dimensions, and the narrow resonance width make this a system of considerable interest as a coherent source of high-frequency phonons.

[1]W. J. Brya and P. E. Wagner, Phys. Rev. 157, 400 (1967).
[2]H-K Liu, R. I. Josephs, and P. E. Wagner, J. Phys. C 5, 828 (1972); 5, 843 (1972).
[3]C. Leonardi and F. Persico, Phys. Rev. B 11, 102 (1975).
[4]W. E. Bron and W. Grill, Phys. Rev. Lett. 40, 1459 (1978).
[5]P. Hu, Phys. Rev. Lett. 44, 41 (1980).
[6]J. E. Rives and R. S. Meltzer, Phys. Rev. B 16, 1807 (1977).
[7]M. M. Broer, J. Hegarty, G. F. Imbusch, and W. M. Yen, Opt. Lett. 3, 175 (1978).
[8]H. Wolfrum, K. Lanzinger, and K. F. Renk, Opt. Lett. 5, 294 (1980).
[9]L. A. Riseberg and H. W. Moos, Phys. Rev. Lett. 19, 1423 (1967).
[10]C. Krischer, Appl. Phys. Lett. 13, 310 (1968).
[11]W. E. Bron, Rep. Prog. Phys. 43, 301 (1980).